An Investigation on the Relationship Between Distortions in the Motion Magnified Videos, and the Choice of Filter Bank

Aral Sarrafi, Zhu Mao
Structural Dynamics and Acoustics Systems Laboratory
Department of Mechanical Engineering
University of Massachusetts Lowell
1 University Avenue, Lowell, MA 01854, USA.
zhu mao@uml.edu, 978-934-5937

ABSTRACT

Phase-based motion magnification is one the most recent advances in computer vision and computational photography that has introduced new approaches for structural dynamics identification. Unwanted artifacts and distortions are often present in the motion-magnified videos that can be traced back to the reconstruction procedure after manipulating the phase variations. Within this article, we have studied this phenomenon more closely to find out the relations between the distortions and the choice of filter bank, and the magnification factor. It has been shown that Fourier transformation can reconstruct motion-magnified frames without inducing any distortions, and on the other hand using other filter banks such as Gabor wavelets will generate motion-magnified frames that have distortions in them. The source of these distortions are also discussed briefly.

Keywords: Video Magnification, Gabor Wavelets, Computer Vision, Computational Photography

1 Introduction

Using digital cameras as a measurement instrument has been gaining more attention in the recent years due to the availability of digital cameras, abundant storage capacity, and faster modern computers [1, 2]. Along with the recent advances from hardware perspective, more elaborate computer vision and computational photography algorithms have emerged in the past few years [3]. Non-contact and full field measurement capability of digital cameras are the main advantages of this powerful approach to sense, measure, and analyze the subjected problem. However, interpreting the variations in pixel values in the acquired images to meaningful parameters from engineering point of view is a more challenging task compared to traditional sensory systems [4, 5]. The procedure of extracting useful information from images or sequence of images is the focus of computer vision, photogrammetry, and computational photography.

Phase-based motion estimation (PME) and Phase-based motion magnification (PMM) are among the most recent advances in computer vision and computational photography that have shown promising results for applications in structural dynamics identification and structural health monitoring [6-8]. Both PMM and PME and are able to capture the imperceptible vibrations in a video recorded from the structure while vibrating [9]. The information provided by PME and PMM enables the engineers to identify important properties of the structures such as resonant frequencies, operating deflection shapes (ODS), and mode shapes. There has been numerous studies on the applications of PMM and PME for variety of structures that can be found in the following references [9-14].

Based on the previous researches, the PME has been used to estimate the resonant frequencies of the structure. Subsequently the PMM has been used to amplify the motion in a narrow frequency band around the estimated resonant frequency from PME to visualize the operating deflection shape of the structure associated with the selected resonant frequency for human vision system.

In general, after applying the PMM (motion magnification) stage the generated video will contain several artifacts and distortions, which will be shown with more details later in this paper. These distortions are undesired, and may introduce uncertainties in the other post-processing stages that will be using the information from the motion-magnified videos. Moreover, experiments have shown that the amount of these undesired distortions increases for larger magnification factors.

The objective of this paper is to investigate the reason behind the arising artifacts, and distortions by taking a closer look at the procedure of generating motion-magnified videos.

In the first section of the paper, different results with the motion-magnified videos are presented to demonstrate arising distortions in the motion magnified videos. The second part of the paper, takes a closer look at the procedure of generating motion-magnified videos, to demonstrate the source of the distortions, and finally the conclusions are presented.

2 Distortions in motion magnified videos

In this section, two different examples of the applications of motion-magnified videos for structural dynamics identification are presented, to demonstrate the distortions in the motion magnified videos. The first application is motion-magnified videos of a lab-scale cantilever beam.

A CMOS high-speed camera shown in Figure 1 captures the sequence of images from the vibrating cantilever-beam. The sequence of images was recorded with a sampling rate of 2500 frames per second, and based on the Nyquist theorem the resonant frequencies and operating deflection shapes can be extracted up to 1250 Hz without facing aliasing. Because there is no anti-aliasing filtering available for optical measurements the aliased higher order frequencies can be detected often, and the post-processing of the data should be handled more carefully.

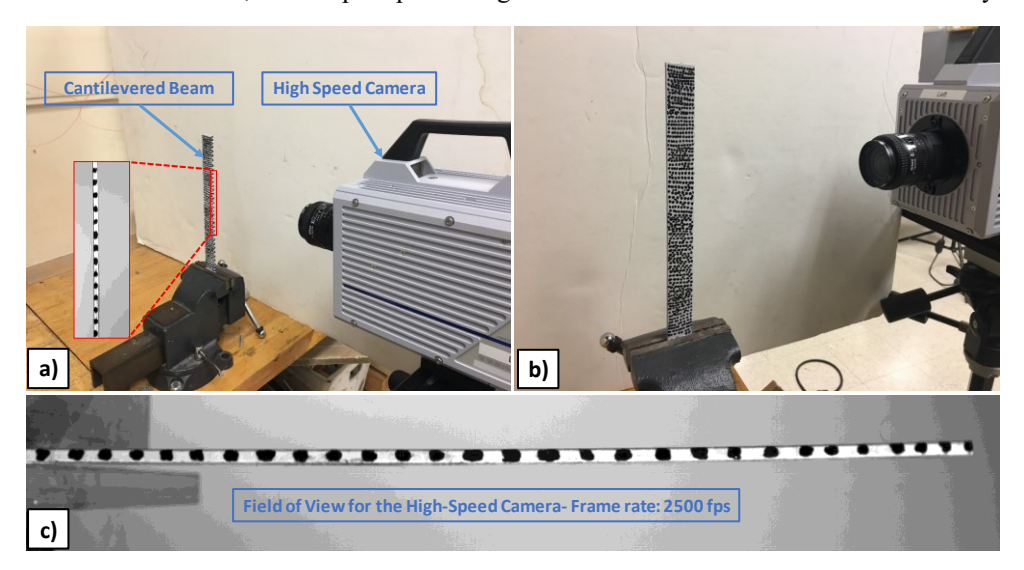


Figure 1. a and b) The CMOS high-speed camera and the cantilever beam, c) field of view for the camera capturing the sequence of images of the vibrating beam[15]

Figure 2 shows the two snaps shots of the motion-magnified video for the second ODS of the cantilevered beam (The resonant frequency associated with second ODS of the beam is about 212.5 Hz). The ellipses in Figure 2 shows the aforementioned distortions that are induced in the phase-based motion magnification procedure. Next, we will show another example of motion magnified videos that includes such distortions in it. Similar distortions can be also found for the other ODSs of the cantilever beam that are not presented here to maintain brevity.

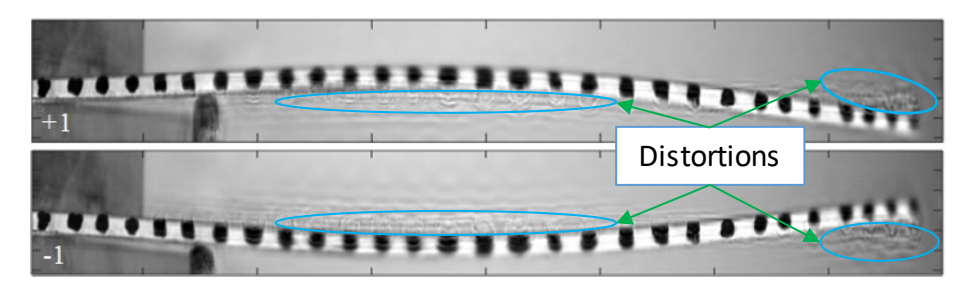


Figure 2. Two snap shots of the motion magnified video for second ODS while the beam is at its maximum deflection- Distortion areas shown with the ellipses [15]

The second example contains the motion-magnified video for a 2.3-meter Skystream® 4.7TM wind turbine blade (WTB).

In order to extract the dynamic behavior of the WTB, the test bed shown in Figure 3 was used. A Skystream® 4.7TM WTB was clamped at the root and excited by a modal hammer providing a force impulse.

The sequence of images/video of the vibrating WTB was captured using a single 4-megapixel (2048×2048 CMOS sensor) PHOTRON® high-speed camera equipped with a 14-mm lens, as shown in Figure 3(b). The dynamic range of the camera pixels are 8 bits and for each pixel an intensity value in the interval [0-255] is assigned. The frame rate of the high-speed camera was set up to record the sequence of images at 500 frames per second (fps). The sequence of images of the vibrating wind turbine blade is measured up to 4 seconds (2000 frames).

Figure 3(c) shows enhanced image data to demonstrate the field of view for the high-speed camera including both the tip and the root. For better visualization in the rest of the article, contrast will be enhanced to better illustrate the testing results. After acquiring vibrational video data from the WTB, PME was used to obtain the resonant frequencies and motion magnification is applied to visualize the operating deflection shapes of the wind turbine blade.

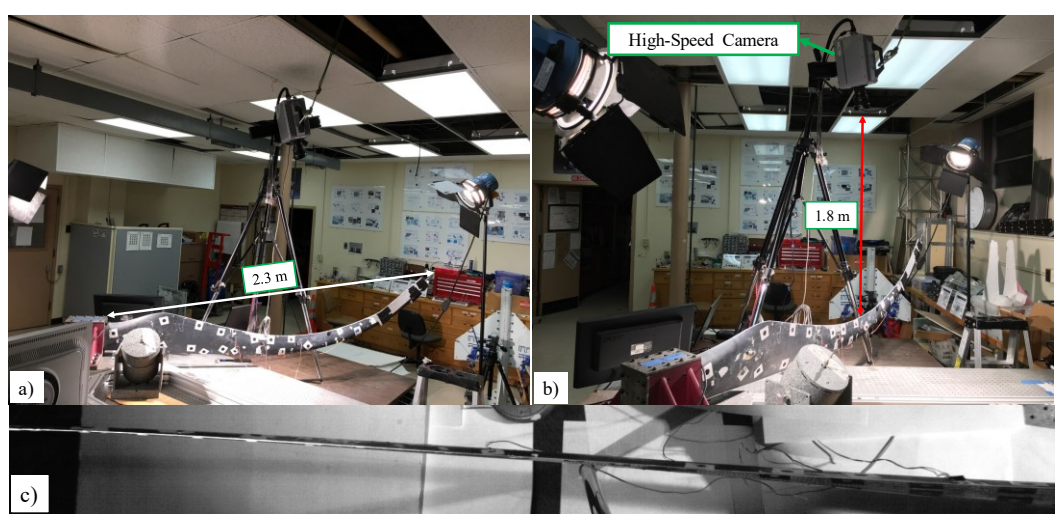


Figure 3. (a) 2.3-m Skystrem® 4.7 cantelivered WTB and the additive mass representing induced damage; (b) Four megapixels PHOTRON high-speed camera equipped with 14-mm lens; (c) Enhanced image data showing the field of view of the high-speed camera [12]

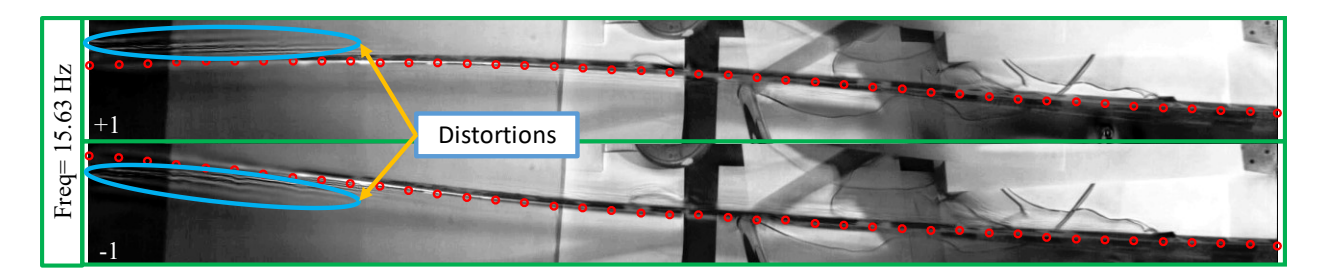


Figure 4. Snap shots of the motion magnified video for the second ODS of the WTB at its maximum deflection— Distortion areas shown with the ellipses

Figure 4 shows two snap shots of the motion-magnified video for the second ODS of the WTB at its maximum deflection. Similar to the previous motion magnified video for the cantilever beam, the results for the second ODS of the WTB also demonstrates the presence of distortions and artifacts in the motion magnified videos. In the next section will briefly discuss the reason causing these distortions.

3 Basic procedure of generating motion magnified videos

In order to understand the source of artifacts and distortions in the motion-magnified videos, we will need to take closer look at the basic mathematics that is governing this procedure. The original motion magnification algorithm uses steerable filters, and Gabor wavelets. Before showing how the Gabor wavelets can be used to generate motion-magnified videos, we will be discussing using Fourier transformation to generate the motion-magnified videos. In reality the Fourier transformation is not a good option for generating motion-magnified videos, because the basis functions for Fourier transformation are Sines and Cosines that have infinite spatial domain, thus they cannot handle local motion in the videos. However, investigating the Fourier transformation can be a good starting point to understand the source of distortions. Moreover, for simplification, we will be discussing only 1-D images, and the argument can be easily expanded to 2-D signals and images. Assuming that motion Δx has been applied to the image the 1-D image can be expressed as $I(x + \Delta x)$. Next, the image can be approximated with Fourier series decomposition [6] as follows

$$I(x + \Delta x) = \sum_{\omega = -\infty}^{\omega = +\infty} A(\omega) e^{i\omega(x + \Delta x)}$$
(1)

As it is clear in the equation (1) changing the phase-values in the Fourier representation of the image, will result in changes in the motion in the spatial domain of the image. For example, if we add $\alpha \Delta x$ to the phase of the Fourier representation we will be having a motion-magnified videos after applying the inverse Fourier transformation.

$$I(x+(1+\alpha)\Delta x) = \sum_{\omega=-\infty}^{\omega=+\infty} A(\omega)e^{i\omega(x+\Delta x+\alpha\Delta x)}$$
(2)

As equation (2) shows the reconstructed image after manipulating the phase in frequency domain will have a larger motion compared to the original image. The following simulation also confirm the results. In this simulation a Gaussian curve is used as our artificial video frame. The second frame is generate by applying a motion to the first frame, and then the motion magnification is performed using the Fourier transformation and the phase manipulation as discussed earlier. As it is clear in the case of using Fourier transformation (sine and cosines as the basis functions), the reconstruction can be performed without the presence of distortions for different magnification factors (α).

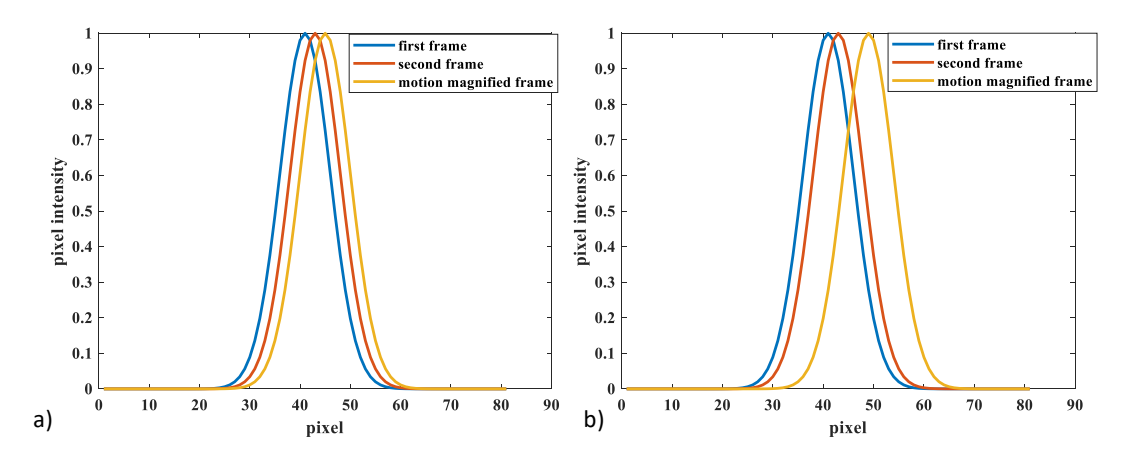


Figure 5. Generating motion magnified frames using Fourier transformation. a) $\alpha = 1$, b) $\alpha = 3$

Although it seems like Fourier transformation can be a good option to generate motion-magnified videos, this approach will fail to process videos with local motion. In reality, all the videos have local motions in them and decomposing the frames to sine and cosine basis functions that have global domain is not feasible. Therefore, other basis functions with local properties should be considered. Gabor wavelets are one of the simplest approaches to this end. Gabor wavelets is a sinusoid that is multiplied by a Gaussian envelope. This Gaussian envelope will cause the Gabor wavelet to have finite spatial domain which suites for processing the local motions. However, once the Gaussian envelope is applied to the sine and cosine basis functions, changing the phase to reconstruct motion-magnified videos will cause the distortions and artifacts to appear in the motion-magnified video. The reason is that in this procedure the amplitude is not changing, while the phase of the basis function is being manipulated. By changing the phase values, the basis function will shift forward under the Gaussian envelope, and the Gaussian envelope forces the basis function to obtain smaller value as it gets closer to the tail of the Gaussian envelope. The simulation also shows that for larger magnification factors (α) the distortions are more severe. This phenomenon is also highly related to the standard deviation of the Gaussian envelope. For Gaussian, envelopes with larger standard deviations larger magnification factors are achievable [6].

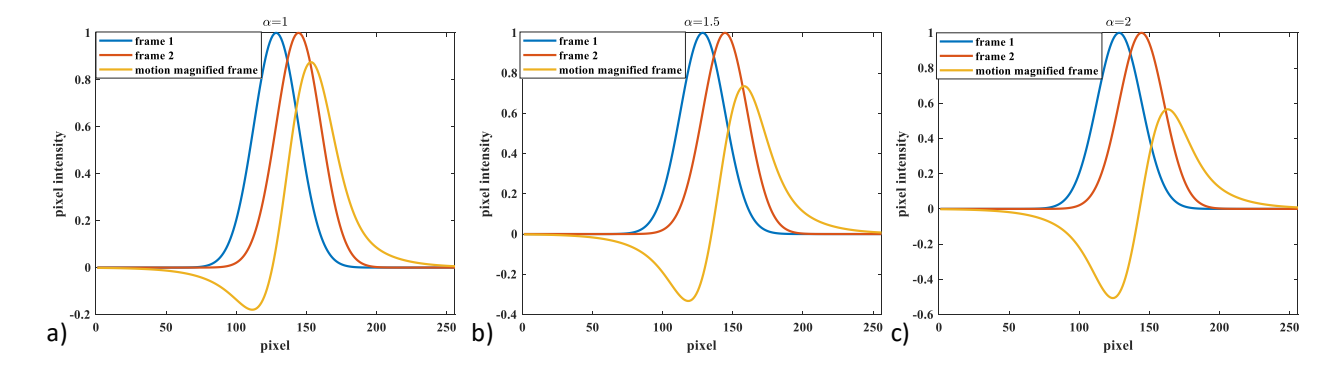


Figure 6. Generating motion magnified videos using Gabor wavelets for different magnification factors.

As it is clear in Figure 6 as the magnification factor increases the basis functions moves further towards the tail of the Gaussian envelope which induces more distortions to the reconstructed motion magnified frame.

4 Conclusions

In this paper, two different motion magnified videos for two structures (cantilever beam and a wind turbine blade) are presented to show the distortions and artifacts that are induced during the phase-based motion magnification procedure. The application of Fourier transformation for motion magnification was discussed briefly, and it has been shown that in case of having global motion the Fourier transformation can reconstruct motion magnified videos without inducing any distortions. However, in reality, the videos have local motions that should be taken care of and Fourier transformation is not a feasible solution. In order to handle these local motions other sets of basis functions with finite spatial domain are used such as Gabor wavelets. Using a Gaussian envelope to limit the spatial domain of the basis functions for local motion processing comes at a cost, which is the induced distortions for larger magnification factors. Changing the phase will make the sine and cosine functions to move towards the tail of the Gaussian envelope, which is the main source of distortions and artifacts in the motion-magnified videos. For future work, use of more adaptable procedure and filter banks can be considered to support larger magnification factors and to reduce the severity of the induced distortions in the motion-magnified videos.

5 Acknowledgement

This material is based upon work supported by the National Science Foundation under Grant No. 1762809. Any opinions, findings, and conclusions or recommendations expressed in this material are those of the authors and do not necessarily reflect the views of the National Science Foundation.

6 References

- [1] D. Feng, M.Q. Feng, Computer vision for SHM of civil infrastructure: From dynamic response measurement to damage detection—A review, Engineering Structures, 156 (2018) 105-117.
- [2] J. Baqersad, P. Poozesh, C. Niezrecki, P. Avitabile, Photogrammetry and optical methods in structural dynamics—A review, Mechanical Systems and Signal Processing, (2016).
- [3] C.-Z. DONG, O. CELIK, F.N. CATBAS, Long-term Structural Displacement Monitoring using Image Sequences and Spatio-Temporal Context Learning, Structural Health Monitoring 2017, (2017).
- [4] J. Javh, J. Slavič, M. Boltežar, The subpixel resolution of optical-flow-based modal analysis, Mechanical Systems and Signal Processing, 88 (2017) 89-99.
- [5] J. Javh, J. Slavič, M. Boltežar, High frequency modal identification on noisy high-speed camera data, Mechanical Systems and Signal Processing, 98 (2018) 344-351.
- [6] N. Wadhwa, M. Rubinstein, F. Durand, W.T. Freeman, Phase-based video motion processing, ACM Transactions on Graphics (TOG), 32 (2013) 80.
- [7] N. Wadhwa, M. Rubinstein, F. Durand, W.T. Freeman, Riesz pyramids for fast phase-based video magnification, US Patent 9,338,331, 2016.
- [8] N. Wadhwa, H.-Y. Wu, A. Davis, M. Rubinstein, E. Shih, G.J. Mysore, J.G. Chen, O. Buyukozturk, J.V. Guttag, W.T. Freeman, Eulerian video magnification and analysis, Communications of the ACM, 60 (2016) 87-95.
- [9] J.G. Chen, N. Wadhwa, Y.-J. Cha, F. Durand, W.T. Freeman, O. Buyukozturk, Modal identification of simple structures with high-speed video using motion magnification, Journal of Sound and Vibration, 345 (2015) 58-71.
- [10] A. Davis, K.L. Bouman, J.G. Chen, M. Rubinstein, F. Durand, W.T. Freeman, Visual vibrometry: Estimating material properties from small motion in video, Proceedings of the IEEE Conference on Computer Vision and Pattern Recognition, 2015, pp. 5335-5343.
- [11] Y. Yang, C. Dorn, T. Mancini, Z. Talken, G. Kenyon, C. Farrar, D. Mascareñas, Blind identification of full-field vibration modes from video measurements with phase-based video motion magnification, Mechanical Systems and Signal Processing, 85 (2017) 567-590.
- [12] A. Sarrafi, Z. Mao, C. Niezrecki, P. Poozesh, Vibration-based damage detection in wind turbine blades using Phase-based Motion Estimation and motion magnification, Journal of Sound and Vibration, 421 (2018) 300-318.

- [13] A. Sarrafi, P. Poozesh, C. Niezrecki, Z. Mao, Applying video magnification for vision-based operating deflection shape evaluation on a wind turbine blade cross-section, Health Monitoring of Structural and Biological Systems XII, International Society for Optics and Photonics, 2018, pp. 106000M.
- [14] A. Sarrafi, P. Poozesh, C. Niezrecki, Z. Mao, Detection of Natural Frequency and Mode Shape Correspondence Using Phase-Based Video Magnification in Large-Scale Structures, Structural Health Monitoring, Photogrammetry & DIC, Volume 6, Springer, 2019, pp. 81-87.
- [15] A. Sarrafi, Z. Mao, Structural operating deflection shape estimation via a hybrid computer-vision algorithm, Health Monitoring of Structural and Biological Systems XII, International Society for Optics and Photonics, 2018, pp. 106002K.